

**Research Article****Inelastic Cyclic Tests of Grade 80 (550 MPa) Bars with Mechanical Splices**Wrya Abdullah <sup>1,\*</sup> , Seyed Sasan Khedmatgozar Dolati <sup>2</sup> , Arjun Basnet <sup>2</sup> <sup>1</sup> Civil Engineering Department, College of Engineering, University of Sulaimani, Sulaymaniyah, 46001, Iraq<sup>2</sup> Department of Civil and Environmental Engineering, Klesse College of Engineering and Integrated Design, University of Texas at San Antonio, Texas, TX 78249, USA

\*Corresponding Author: Wrya Abdullah, E-mail: Wrya.faraj@univsul.edu.iq

Article Info	Abstract
Article History	This study addresses low-cycle fatigue performance of high-strength steel reinforcement bars (HSRB) when used with mechanical couplers due to the growing demand for higher-strength steel reinforcement bars in both seismic and non-seismic applications, driven by the need to reduce bar congestion, lower material quantities, and consider economic and environmental factors. Low-cycle fatigue involves material failure owing to a finite number of load or deformation cycles, generally occurring under substantial strain rates that surpasses the yielding limit. The experimental program assesses the fatigue behavior of HSRB produced using microalloying, quenching, and tempering techniques, coupled with mechanical couplers (eleven different types) from five companies in the United States of America. The study highlights significant differences in fatigue endurance based on the type and make of couplers and suggests potential improvements in manufacturing processes to enhance fatigue resistance. It is found that the mechanical couplers sustain a loading protocol of (-1% to 3%) when there is a clear distance of 2 times the diameter of the bar between the coupler and the gripping machine from top to bottom. The coupled bars sustained a minimum of 6 half cycles and a maximum of 38 half cycles.
Received May 19, 2024	
Revised Jun 01, 2024	
Accepted Jun 03, 2024	
<b>Keywords</b>	
Inelastic test	
Grade 80 bars	
Mechanical splices	
Fatigue tests	
Couplers	



**Copyright:** © 2024 Wrya Abdullah, Seyed Sasan Khedmatgozar Dolati and Arjun Basnet. This article is an open-access article distributed under the terms and conditions of the Creative Commons Attribution (CC BY 4.0) license.

**1. Introduction**

There is a growing demand for higher-strength steel reinforcement bars in seismic and non-seismic applications owing to the necessity of the reduction in the bar congestion, lower material quantities, and considerations related to economics and the environment [1]. While previous efforts have focused on testing high-strength reinforcing bars (HSRB) monotonically, such as finding fracture strain rates and inelastic hardening, this study explores the low-cycle fatigue endurance of HSRB with mechanical couplers. Low-cycle fatigue refers to a material failure during fatigue testing owing to loading the material cyclically to strain rates large enough that cause the failure with small number of loads or strain cycles [2].

Researchers investigated the usage of HSRB in concrete beams and joints [3–5]. For instance, Zhao et al. investigated the bending behavior of reinforced concrete beams with HSRB after exposing the specimens to elevated temperatures and testing twelve beams [4]. They examined the effects of various factors, including exposure temperatures ranging from room temperature to 1000 °C with an increment of 200 °C, exposure duration of 0 to 2 hours with an increment of 1 hour, yield strengths of (500 and 600 MPa), and the number of heated sides were changing between 2 and 3 sides. The effects of the testing parameters were tested on the bending behavior of the beams, focusing on failure mode, and load-deflection response. Their results indicated that flexural capacities remained largely unchanged at temperatures below 600 °C but decreased significantly when temperatures surpassed 800 °C. Specifically, the ultimate load capacities of beams with HRBS 600 MPa bars exposed to 800 and 1000 °C dropped by 12.9% and 38.7%, respectively, compared to those at room temperature. Prolonged holding times (2 hours) also resulted in a more substantial reduction in flexural capacities, with peak loads decreasing by 2.4% and 9.4% for 0 and 1-hour holding times, respectively.

Other researchers investigated high-strength steel bars in columns [6-9]. Cai et al. [7] examined the seismic behavior of concrete columns that incorporate recycled coarse aggregates (RCA). Tests were conducted on three full size columns with a side length of 600 mm. Key parameters studied include the axial load ratio (ALR) and the use of external confinement of CFRP combined with spiraled groove ultra-high-strength steel bars (UHSSBs) with a nominal yield strength of 1400 MPa. The specimens were subjected to lateral cyclic displacement control and concurrent axial loads. Their results showed that RCA concrete columns, when equipped with both CFRP jackets and UHSSBs, maintained positive lateral stiffness at a 4% drift and exhibited less residual drift compared to traditional ductile columns. Additionally, an increase in ALR resulted in higher residual drift.

Therefore, due to limited data on HSRB with mechanical couplers [2], [10, 11], this study investigates the low-cycle fatigue behavior of HSRB coupled with mechanical couplers. It examines HSRB produced using the two manufacturing techniques in the United States: microalloying, quenching, and tempering. It is an experimental investigation conducted to assess the fatigue performance of these high strength reinforcing bars (HSRB) with mechanical couplers. Furthermore, the findings from this study offer crucial insights and data that can be instrumental in formulating material specifications tailored to the seismic demands of HSRB with mechanical splices, contributing to the development of a seismic-grade standard for these innovative reinforcing bars.

In summary, this experimental study was conducted to compare the fatigue behavior of high strength reinforcing bars with mechanical couplers, highlighting differences in fatigue life and potential improvements in manufacturing processes.

There is an ongoing effort to develop new high strength reinforcing steel bars, motivated by factors such as ease of use, economic considerations, and environmental concerns [12]. To better understand their performance with mechanical couplers, an experiment was conducted to compare the fatigue characteristics of these high-strength bars (HSRB). The research highlighted potential enhancements in the coupler manufacturing processes that could boost the fatigue resistance of high-strength bars with mechanical couplers. The research outcomes also offer valuable insights for the formulation of material specifications tailored for a seismic-grade version of high-strength reinforcing steel bars.

The demand for stronger and more resilient structures in the case of dynamic loadings, such as earthquakes or severe weather conditions, has prompted the exploration of advanced construction materials and techniques [13, 14]. Grade 80 (550 MPa) bars, characterized by higher yield strength, are a promising solution to address the need for improved structural performance. Mechanical splices offer advantages in terms of construction speed, reduced congestion, and increased flexibility in design. While the individual merits of Grade 80 (550 MPa) bars and mechanical splices have been studied independently, the combined behavior of these elements under inelastic cyclic loading conditions requires further investigation. Inelastic cyclic tests serve as a critical tool to assess the ductility, strength, and energy dissipation capacity of reinforced concrete structures subjected to severe and repeated loading. Understanding the performance of Grade 80 (550 MPa) bars with mechanical splices in such conditions is essential for ensuring the resilience of structures in earthquake-prone regions and other high-stress environments. Therefore, the aim of the study is to investigate the HSRB with mechanical couplers inelastically under the strain control loading.

## 2. Materials and Methods

Eleven types of couplers are used in this study produced by five different companies in the United States. The description of the coupler and their company names are coded by the letter “C” and listed in Table 1. Most of the couplers are joined using taper thread, which employs an internally threaded sleeve, to connect bars [15]. To make this, the ends of the bars need to be threaded and prepared to match the design of the couplers. Three couplers are grouted sleeve couplers, which are composed of three primary components: a sleeve, grout, and two openings, including a grout inlet and a grout outlet [3]. The procedure involves equally inserting the bars into the sleeve, followed by filling the sleeve with non-shrink, high-strength grout [16]. One of the couplers was a taper-threaded and swaged coupler. In this technique, the process begins by inserting the bars into a sleeve made of mild steel, and then a hydraulic press machine is used to exert pressure [17]. The application of lateral force on the sleeve causes it to undergo deformation, effectively closing the spaces between the ribs of the bars. When these connected bars are subjected to tensile forces, the friction generated by the deformed sleeve and the ribs of the bars plays a crucial role in

transferring stress and, as a result, prevents the bars from experiencing debonding. Figure 1 shows all the couplers used in this study and emphasizes their length differences. Their length varies between 3 inches (76.2 mm) and 15.5 inches (393.7 mm).

**Table 1.** Types of couplers used in the study.

Company	Description
C1	Swaged/Taper Threaded butt splice
C2	Threaded Rebar butt splice
C3	Taper Threaded
C4	Friction Forged, tapered threaded
C5	Tapered threaded
C6	Grouted connection, tapered threaded
C7	Mechanical Butt-Splice. Align the male-threaded coupler component, the female-threaded coupler component, and the reinforcing bars with upset heads. Installation allows pre-bent and/or pre-tied reinforcing bars to be installed without rotating the bars.
C8	Tapered thread, butt splice
C9	
C10	Grout Splice Coupler
C11	

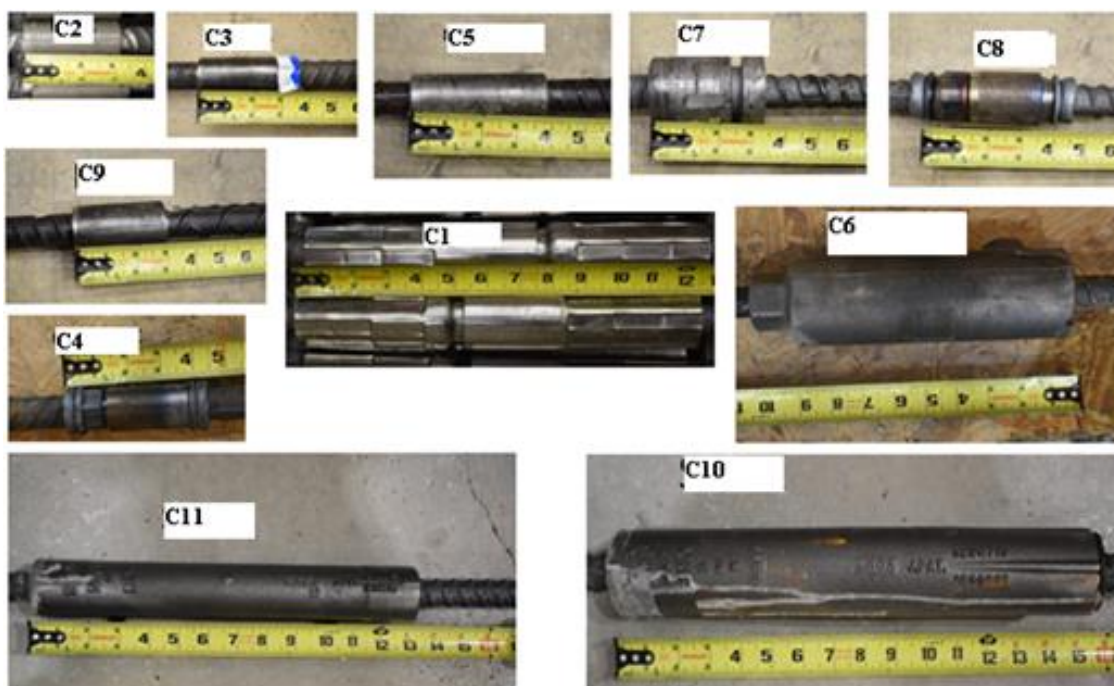


**Figure 1.** Coupler types used in the study.

In this study, the investigation focused on the utilization of two distinct bar types, namely microalloying (MA) and quenching and tempering (QST). Notably, the study was constrained in terms of bar size, limiting it specifically to #8 bars with a diameter of one inch (25 mm) [18]. The selected bars were Grade 80 (550 MPa) and adhered strictly to the specifications outlined by the American Society for Testing and Materials (ASTM) 706 standards.

## 2.1. Machines Used

A universal testing machine from MTS with a capacity of 270 kip (1200 KN) was used for testing the coupled bars. The ultimate speed of the instrument is 11 inches per second, even though strain control was used for testing with different speed rates. A Digital Image Correlation (DIC) system was used to monitor different target points on the bars during the tests and calculate strain, displacement, slip, and other properties between any two points on the bars. After scraping off the surface of the bar, glue was used to attach the paper targets on the bars at the specified locations shown in Figure 2. A unique pattern was printed on a piece of paper, and then the targets were cut to a size of approximately 0.25 inches (6.35 mm) then placed on the bars. Seven targets were mounted on each of the coupled bars before testing, while nine targets were selected in the software to increase the accuracy of monitoring the top and bottom targets. Two sets of targets were essential in calculating the strain between any two points. Several trials were made to find the correct set that can represent the actual strain of the bars and the couplers in between. First, only the targets on the top parts of the couplers were monitored. After that, the targets on the bottom parts were monitored. After a few trails and testing many coupled bars, two sets of targets were used to monitor the strain, which were (0, and 6) and (2, and 8) to count for the strain of the couplers along with the top and bottom strain of the bars. The total length of the bar from the edge of the coupler to the end of the bar was 6.75 inches (171.45 mm), where 2 inches (50 mm) represented the clear gripping distance between the edge of the coupler and the edge of the gripped part, and the remainder was gripped inside the machine. The decisive factor in restricting the distance to those 2 inches (50 mm) was the buckling of the coupled bars during testing. Therefore, several trails were made before the final gripping distance of 2 inches (50 mm).

## 2.2. Testing Parameters

### 2.2.1. Gripping Distance

The gripping distance is the distance between the end of the coupler to the location of the grip in the machine which affects the behavior of the bars during testing. To avoid buckling during testing, different gripping distances are tested.

The gripping distance of  $2 db$ , where  $db$  is the diameter of the bar, was used to avoid buckling. This distance is selected after testing different gripping distances ranging from  $4 db$  to  $2 db$ , but the failure mode in the larger couplers was buckling of the bars, which led to a loss of the number of targets on the coupled bars, as shown in Figure 3.

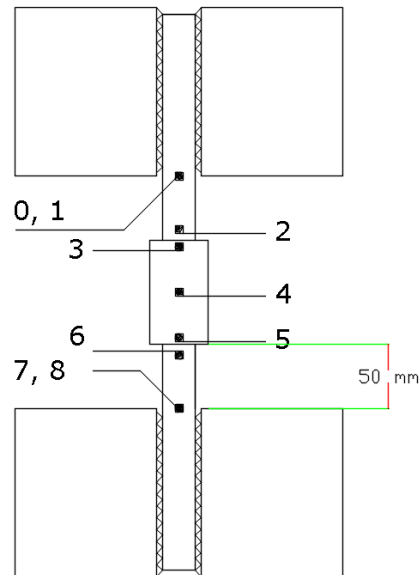


**Figure 2.** A coupled bar in between the grips of the machine with the targets.

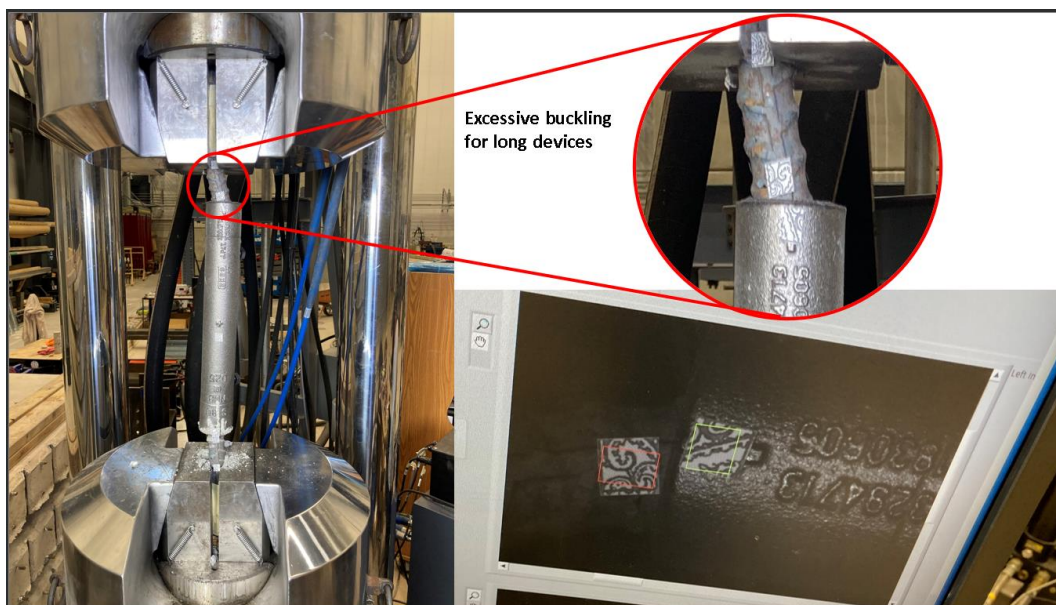


**Figure 3.** Excessive buckling of long couplers and losing targets in the DIC system.

### 2.2.2. Loading Protocol

The tests were carried out under strain control of (-1% to 3%) with a speed rate of 0.012 Hz. This strain range was selected based on avoiding buckling in the couplers, as other strain ranges were checked but resulted in buckling of the coupled bars. Therefore, the specimens were loaded until the strain between the two targeted points reached 3% in tension and then loaded in compression until that strain became -1%.

### 2.2.3. Testing Procedure:

To conduct the experimental phase, a minimum of three bars underwent strain-controlled testing until reaching failure. The bars were precisely cut to the specified length, with a primary segment measuring 4.75 inches (120.65 mm) for engagement with the gripping machine, and a secondary length of 2 inches (50 mm), representing the distance from the coupler's edge to the gripping machine. Consequently, the variability in specimen length stemmed from the non-uniform coupler lengths. Subsequently, targets were affixed to the bar's surface at seven distinct locations, as illustrated in Figure 2. The specimens were then securely gripped from both ends by applying a pressure of 7000 psi (48.26 MPa). The speed of the testing was affixed to 0.012 HZ for all the specimens, and the test continued until observable failure occurred in the specimens.

## 3. Results and Discussions

### 3.1. Bare Bars:

A typical stress strain of the bare bars is shown in Figure 4. Strength degradation is present in the QST bars but not in the MA bars. This can be observed even in bars with couplers. Both of the bars reached the ultimate stress of 100 ksi (689 MPa), which is 1.25 times the yielding stress of 80 ksi (550 MPa) based on ASTM 706.

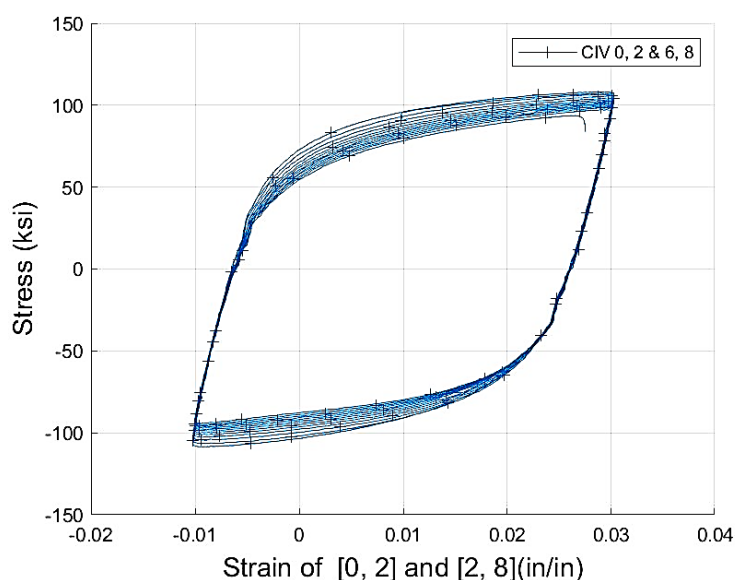


**Figure 4.** Typical stress-strain of the bare bars.

A typical fracture plane of both bar types is shown in Figure 5. A similar fracture plane is observed in all the bars with mechanical couplers, where the MA bars fail as a straight plane while the QST bars fail with an angle.



(a) QST bar fracture plane



(b) MA bar fracture plane

**Figure 5.** Bare bar fractures.

### 3.2. Bars with Couplers

#### 3.2.1. Number of Half Cycles to Failure

The total number of half cycles to the failure of each specimen was measured and is presented in Table 2. Coupler C11 resisted the maximum number of half cycles of 38, while coupler C2 resisted the minimum number of half cycles due to the loss of their threads. It is worth mentioning that the strain rates are higher than those set by AC133 [19].

**Table 2.** Low cyclic test results

Specimens tested	MA Number of half-cycles	QST Number of half-cycles
C2	12	2 (lost threads)
C3	10	NA
C9	6	6
C8	20	18
C7	18	NA
C5	10	26
C11	38	NA

#### 3.2.2. Stress-Strain of The Bars

A typical stress-strain of the coupled bars is shown in Figure 6, where the strain goes from -1% to 3% and the maximum stress varies between -100 ksi (-689 MPa) and 100 ksi (689 MPa). The bars do not possess a clear yield stress as these are high-strength steel bars [20]. It was noted that the bars fractured in the tension eventually after a complete cycle.

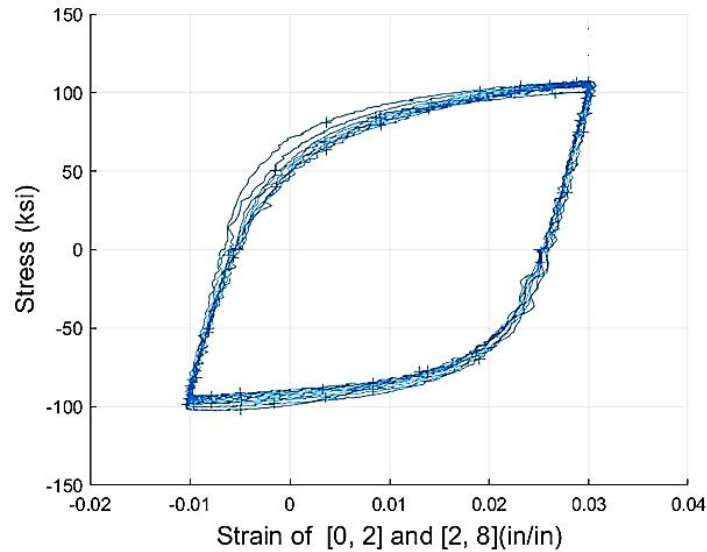


**Figure 6.** Stress-strain of bar coupled with the mechanical coupler of C7.

### 3.2.3. Top and bottom bar strains

It was found that there is a difference between the top and bottom parts of the bars in all the specimens tested. The machine was pulling the coupled bars from the top, which means that only the top part of the machine was moving during the test. Figure 7 shows a typical stress-strain diagram of the top and bottom bars with the coupler. The strain of the bottom bar was greater than that of the top bar, where it was moving from (-1%) to (3%) while the average strain was the same as shown in Figure 6. This was not the case for all the couplers as in some of them, the top part strain was greater than that of the bottom part.

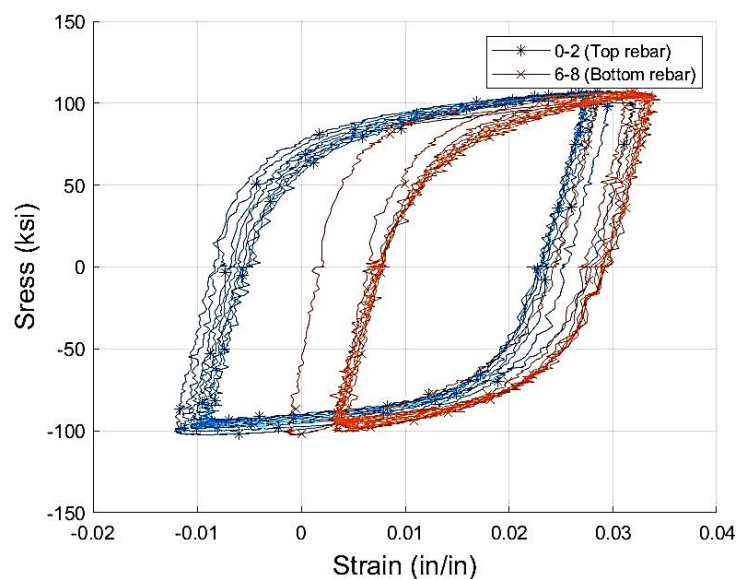
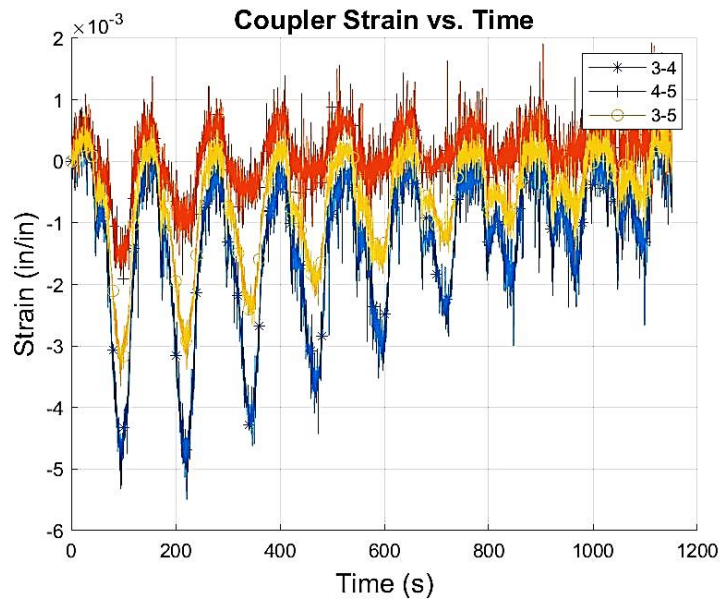


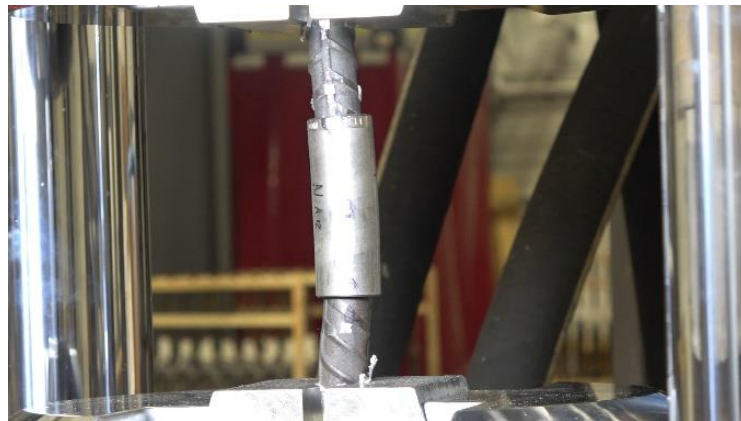
**Figure 7.** Top and bottom bar stress-strain comparison of coupler C7.

### 3.2.4. Coupler Strain

The strain on the couplers was monitored, and it was found that there is enough strain on the couplers to cause their yielding. Figure 8 (a) shows the coupler strain, which was at the top of -0.5%, which is beyond the yielding strain of 0.275% for a high-strength steel of grade 80 (550 MPa). This was the reason behind the visible bent in the couplers as shown in Figure 8 (b).



(a) Stress-strain of the mechanical coupler C7.



(b) Visible bending of mechanical coupler C5

**Figure 8.** Coupler strain and bending of C7.

### 3.2.5. Coupler Slip

Figure 9 shows the slip of the coupler C7, which was prevalent in all the couplers and consisted of two separate parts. There was a maximum slip of more than 0.1 inch (2.54 mm) in the upper part of the coupler.

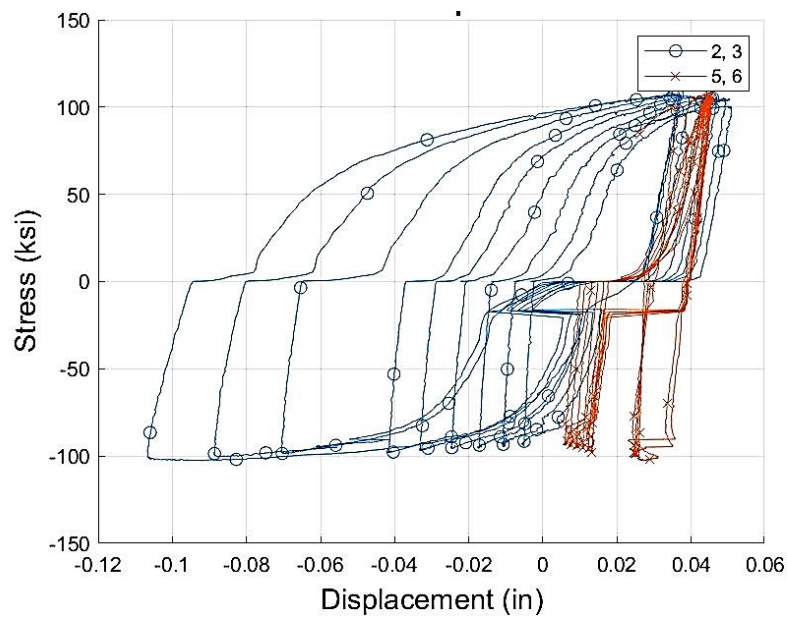


**Figure 9.** Coupler C7 slip.

### 3.2.6. Failure Mode

All of the failures occurred in the bars, either on the upper part of the coupled bar or the lower part. Some of the coupled bars failed at the junction between the coupler and the bar, as shown in Figure 10, while others failed in between the coupler and the grip of the machine, as shown in Figure 11.



**Figure 10.** Fracture of the coupled bar with mechanical coupler C3



**Figure 11.** Fracture of the coupled bar with a mechanical splice of C7.

Figure 12 (a)-(d) shows the failure mode of the other couplers fractured in the bars. The buckled bars with couplers are not shown.



(a) Fracture of coupler C2



(b) Fracture of coupler C5



(c) Fracture of coupler C8



(d) Fracture of coupler C9

**Figure 12.** Fracture of couplers

#### 4. Conclusion

From the current study, it can be concluded that the coupled bars of grade 80 (550 MPa) can sustain a loading protocol ranging from a strain rate of -1% to 3%, with most of the couplers withstanding a minimum of six half cycles without failure. Additionally, all the couplers successfully met the elastic limits set

by AC133. During inelastic cyclic testing, the upper part of the coupled bar exhibits different strain compared to the lower part. Also, the couplers yield under a loading strain rate of -1% to 3%, as the strain in the coupler surpasses the yielding strain. A clear distance of twice the bar diameter between the edge of the coupler and the gripping machine leads to buckling failure in couplers longer than 10 inches (254 mm). Finally, fracture occurs in the bar, either at the junction or between the coupler and the gripping machine.

**Acknowledgement:** We acknowledge the support from the University of Texas at San Antonio and the Large-Scale Testing Lab.

**Funding:** This study was sponsored by The Charles Pankow Foundation, The Concrete Reinforcing Steel Institute, and The American Concrete Institute's Concrete Research Council.

**Declaration of Competing Interest:** The authors declare that they have competing of interest for the products tested which were provided and sponsored by the companies. Therefore, the company names are hidden.

## References

- [1] NEHRP, 2014, *Use of High-Strength Reinforcement in Concrete Structures*. National Institute of Standards and Technology, California, United States.
- [2] D. Wu, Y. Ding, J. Su, Z. X. Li, and L. Zong, Investigation on low-cycle fatigue performance of high-strength steel bars including the effect of inelastic buckling, *Eng. Struct.*, vol. 272, no. April, p. 114974, 2022, doi: 10.1016/j.engstruct.2022.114974.
- [3] Y. Zheng, M. Xie, Z. Liu, Y. Zhang, and X. Ding, Performance of high strength steel bar splice with novel grouted deformed sleeve under tensile load, *Constr. Build. Mater.*, vol. 403, no. August, p. 133092, 2023, doi: 10.1016/j.conbuildmat.2023.133092.
- [4] J. Zhao, Y. Jiang, and X. Li, Flexural behavior of concrete beams reinforced with high-strength steel bars after exposure to elevated temperatures, *Constr. Build. Mater.*, vol. 382, no. January, p. 131317, 2023, doi: 10.1016/j.conbuildmat.2023.131317.
- [5] C. Kim, S. Kim, K.-H. Kim, D. Shin, M. Haroon, and J.-Y. Lee, Torsional Behavior of Reinforced Concrete Beams with High-Strength Steel Bars, *ACI Struct. J.*, vol. 116, no. 6, Nov. 2019, doi: 10.14359/51718014.
- [6] M. L. Zhuang, C. Sun, and B. Dong, Experimental and numerical investigations on seismic performance of HTRB630 high-strength steel bars reinforced concrete columns, *Case Stud. Constr. Mater.*, vol. 17, no. May, p. e01185, 2022, doi: 10.1016/j.cscm.2022.e01185.
- [7] R. Cai, J. Zhang, Y. Liu, and X. Tao, Seismic behavior of recycled concrete columns reinforced with ultra-high-strength steel bars, *Eng. Struct.*, vol. 279, no. January, p. 115633, 2023, doi: 10.1016/j.engstruct.2023.115633.
- [8] Y. Zhang, X. Xiong, L. He, X. Zhang, and M. He, Behavior of large-scale concrete columns reinforced with high-strength and high-toughness steel bars under axial and eccentric compression, *J. Build. Eng.*, vol. 79, no. August, p. 107766,

- 2023, doi: 10.1016/j.jobe.2023.107766.
- [9] J. Zhang, R. Cai, C. Li, and X. Liu, Seismic behavior of high-strength concrete columns reinforced with high-strength steel bars, *Eng. Struct.*, vol. 218, p. 110861, Sep. 2020, doi: 10.1016/j.engstruct.2020.110861.
- [10] R. Anggraini, Tavio, I. G. P. Raka, and Agustiar, Stress-strain relationship of high-strength steel (HSS) reinforcing bars, *AIP Conference Proceedings*, 2018, p. 020025, doi: 10.1063/1.5038307.
- [11] Tavio, R. Anggraini, I. G. P. Raka, and Agustiar, Tensile strength/yield strength (TS/YS) ratios of high-strength steel (HSS) reinforcing bars, *AIP Conference Proceedings*, 2018, p. 020036, doi: 10.1063/1.5038318.
- [12] X. Li, J. Zhang, and W. Cao, Hysteretic behavior of high-strength concrete shear walls with high-strength steel bars: Experimental study and modelling, *Eng. Struct.*, vol. 214, p. 110600, Jul. 2020, doi: 10.1016/j.engstruct.2020.110600.
- [13] A. Basnet and R. Suwal, Seismic Vulnerability Assessment of Reinforced Concrete Skewed Bridge Pier Using Fragility Curve, *Invent. J. Res. Technol. Eng. Manag.*, vol. 3, no. 6, pp. 98–107, 2019.
- [14] N. Giordano et al., Life-Cycle Analysis of Incremental Seismic Retrofitting of Traditional Constructions in Nepal, *Int. Conf. Reconstr. Natl. Reconstr. Authority*, 27-29 November, Nepal., 2020.
- [15] D. V. Bompa and A. Y. Elghazouli, Monotonic and cyclic performance of threaded reinforcement splices, *Structures*, vol. 16, no. October, pp. 358–372, 2018, doi: 10.1016/j.istruc.2018.11.009.
- [16] J. Liu, D. Li, and X. Cui, Research status and future directions of defect detection in grouted splice sleeves: A review, *Constr. Build. Mater.*, vol. 402, no. May, p. 133010, 2023, doi: 10.1016/j.conbuildmat.2023.133010.
- [17] H. Dabiri, A. Kheyroddin, and A. Dall'Asta, Splice methods used for reinforcement steel bars: A state-of-the-art review, *Constr. Build. Mater.*, vol. 320, no. December 2021, p. 126198, 2022, doi: 10.1016/j.conbuildmat.2021.126198.
- [18] M. M. Kashani, S. Cai, S. A. Davis, and P. J. Vardanega, Influence of Bar Diameter on Low-Cycle Fatigue Degradation of Reinforcing Bars, *J. Mater. Civ. Eng.*, vol. 31, no. 4, pp. 1–9, 2019, doi: 10.1061/(asce)mt.1943-5533.0002637.
- [19] AC133-1209-R1, Acceptance Criteria for Mechanical Connector Systems for Steel Reinforcing Bars, *International Code Council*, no. 800, pp. 1–9, 2010.
- [20] M. Elices, M. Perez-Guerrero, M. Iordachescu, and A. Valiente, Fracture toughness of high-strength steel bars, *Eng. Fract. Mech.*, vol. 170, pp. 119–129, 2017, doi: 10.1016/j.engfracmech.2016.12.001.